Science Advances
AAAS

advances.sciencemag.org/cgi/content/full/6/12/eaaz0368/DC1

Supplementary Materials for

Regulation of body length and bone mass by Gpr126/Adgrg6

Peng Sun, Liang He, Kunhang Jia, Zhiying Yue, Shichang Li, Yunyun Jin, Zhenxi Li, Stefan Siwko, Feng Xue, Jiacan Su*, Mingyao Liu*, Jian Luo*

*Corresponding author. Email: jluo@bio.ecnu.edu.cn (J.L.); myliu@bio.ecnu.edu.cn (M.L.); jiacansu@126.com (J.S.)

Published 20 March 2020, *Sci. Adv.* **6**, eaaz0368 (2020)
DOI: 10.1126/sciadv.aaz0368

This PDF file includes:

Figure S1

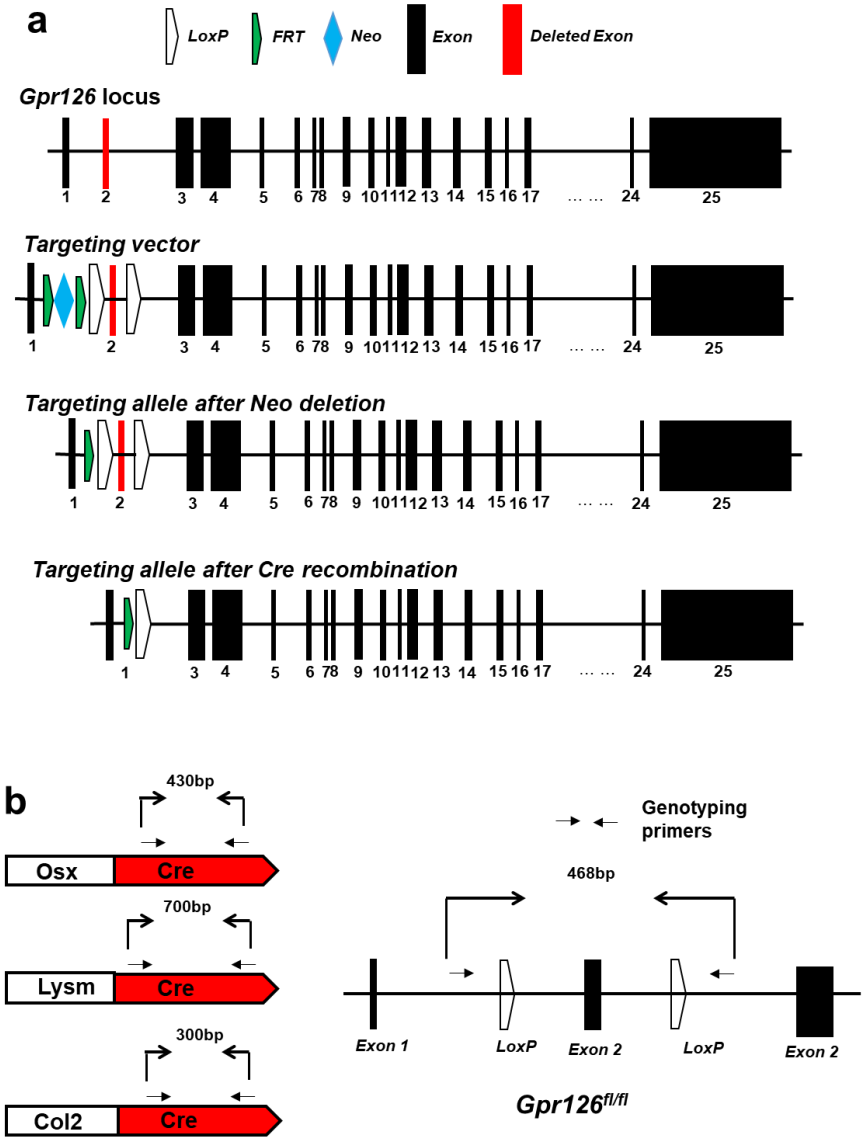

Fig. S1. Strategy of targeting the *Gpr126*^{flox} allele. (**a**) Genomic structure of the wild type murine *Gpr126* gene, the targeting vector and the targeted alleles are indicated. Exon 2 was flanked by *LoxP* sequences (blank pentagon); the Neo cassette was flanked by *frt* sites (green pentagon). The modified *Gpr126* locus after homologous recombination (Neo+allele), and the deleted *Gpr126* gene after Cre-mediated excision of exon 2 are shown. (**b**) The design of primers for mouse genotyping.

Figure S2

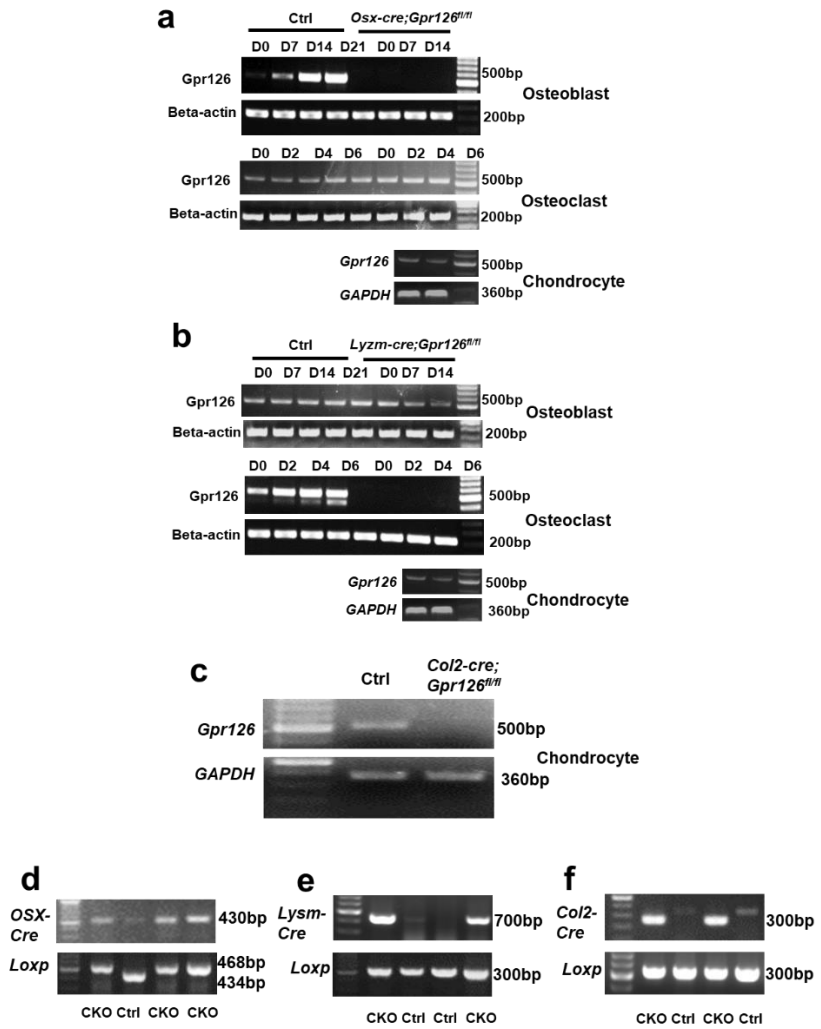

Fig. S2. The expression of *Gpr126* in different bone cells and genotyping. (**a**) Representative gel showing Gpr126 expression in BMSCs undergoing osteoblast differentiation, and BMMs undergoing osteoclast differentiation, and chondrocytes from articular cartilage from control (Ctrl) and *Osx-cre;Gpr126*$^{fl/fl}$ mice, respectively. (**b**) Representative gel showing Gpr126 expression in BMSCs undergoing osteoblast differentiation, and BMMs undergoing osteoclast differentiation, and chondrocytes from articular cartilage from *Gpr126*$^{fl/fl}$ (Ctrl) and *Lysm-cre;Gpr126*$^{fl/fl}$ mice, respectively. (**c**) Representative gel showing Gpr126 expression in chondrocytes from *Gpr126*$^{fl/fl}$ (Ctrl) and *Col2-cre;Gpr126*$^{fl/fl}$ mice articular cartilage, respectively. (**d-f**) Representative gel showing the genotypes for the *Gpr126* conditional knockout in osteoblasts (434 bp PCR product for Loxp (Ctrl) mice, while 468 bp for CKO mice) (d), osteoclasts (e) and chondrocytes (f), respectively.

Figure S3

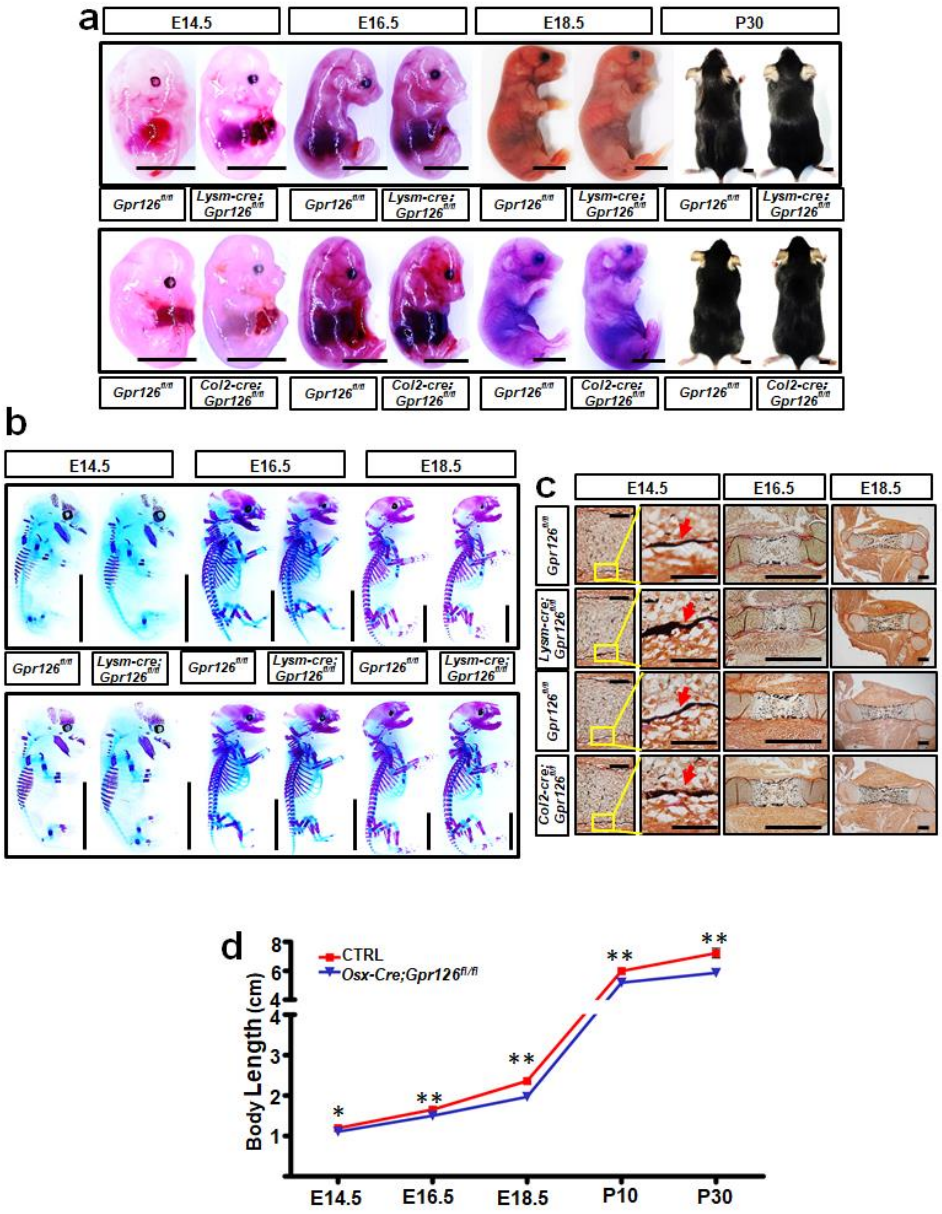

Fig. S3. Body length and embryonic bone formation in *Lysm-Cre;Gpr126*$^{fl/fl}$ and *Col2-Cre;Gpr126*$^{fl/fl}$ was not different compared to their control littermates. (**a**) Images of body size at E14.5, E16.5, E18.5, and P30 of *Lysm-Cre;Gpr126*$^{fl/fl}$ (top), *Col2-Cre;Gpr126*$^{fl/fl}$ (bottom) and control littermates. Scale bars, 5 mm. (**b**) Whole skeletal preparation of *Lysm-Cre;Gpr126*$^{fl/fl}$ (top), *Col2-Cre;Gpr126*$^{fl/fl}$ (bottom) mice, and Ctrl littermates at E14.5, E16.5, and E18.5. Scale bars, 5 mm. (**c**) Von Kossa staining analysis for bone mineralization in E14.5 (left), E16.5 (middle), and E18.5 (right) embryonic femurs of *Lysm-Cre;Gpr126*$^{fl/fl}$ (top), *Col2-Cre;Gpr126*$^{fl/fl}$ (middle), and Ctrl littermates. Scale bars, 100 μm (at E14.5 left), 50 μm (at E14.5 right) & 1 mm (at E16.5 & E18.5). (**d**) Body length was determined by measuring nasal-to-anal distance using a caliper after anesthesia in *Osx-Cre*;*Gpr126*$^{fl/fl}$ mice and Ctrl littermates at E14.5, E16.5, E18.5, P10, and P30. Bars represent mean ± SD. *p < 0.05; **p < 0.01. n =2/group/time point. Photo credit: Peng Sun, East China Normal University

Figure S4

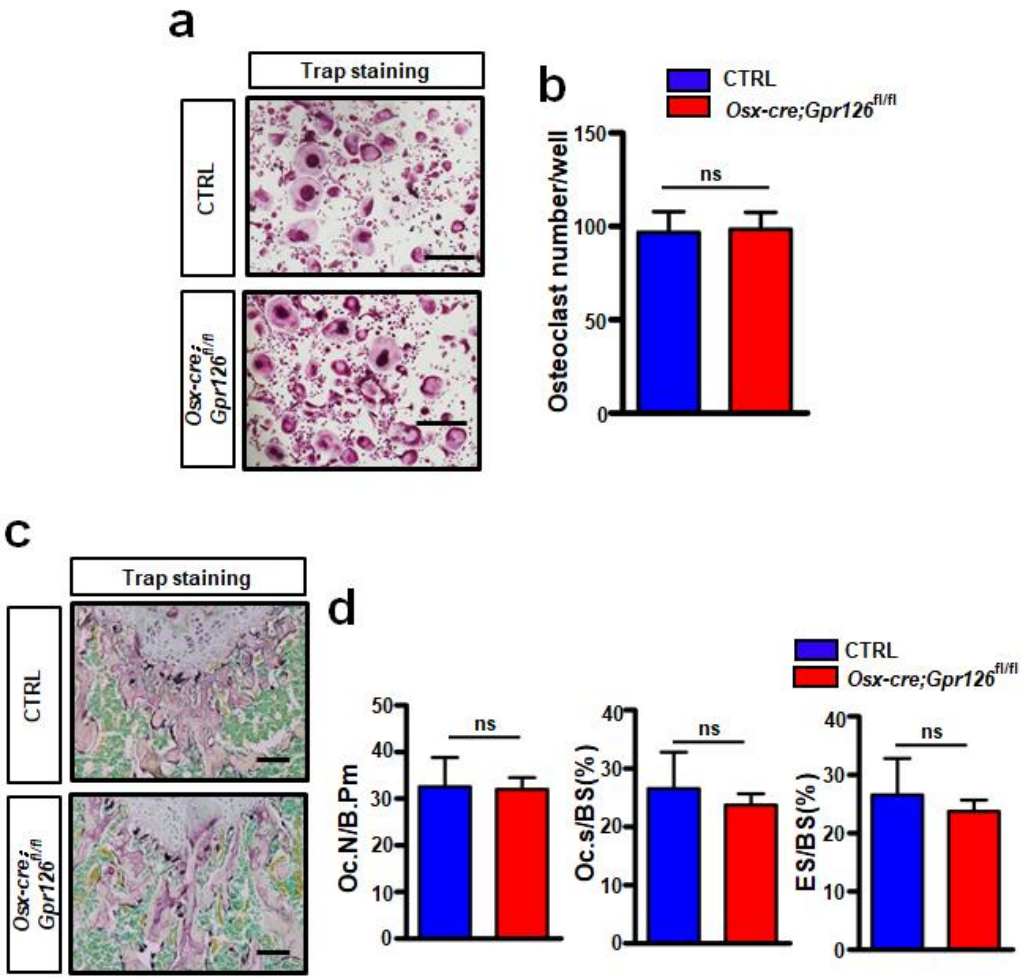

Fig. S4. Deletion of *Gpr126* in osteoblast lineage (Osx-Cre) had little effect on osteoclastogenesis and osteoclast activity in vivo and in vitro. (**a**) Representative images of TRAP positive cells generated from bone marrow cells cultured with M-CSF and RANKL incubation for 6 days. Scale bars, 250 μm. (**b**) Quantification of TRAP-positive cells (> 3 nuclei) from 96-well plates. ns, not significant. n=6. (**c**) Representative images of TRAP staining of femur histological sections from 6-week-old mice. Scale bars, 250 μm. (**d**) The number of osteoclasts/bone perimeter (N.Oc/B.Pm), osteoclast surface/bone surface (Oc.S/BS), and the eroded surface/bone surface (ES/BS) were analyzed with the OsteoMeasure Analysis System. ns, not significant. n=5.

Figure S5

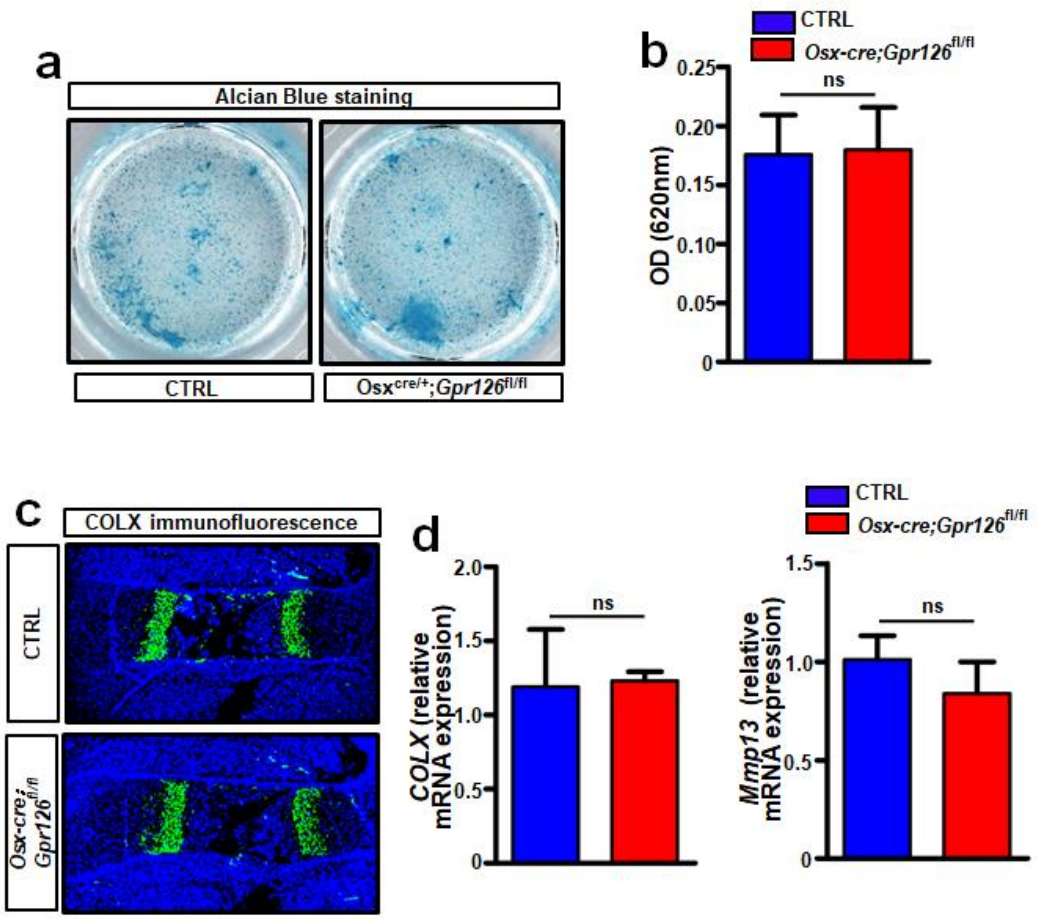

Fig. S5. Deletion of *Gpr126* in osteoblast lineage (Osx-Cre) had little effect on chondrocyte differentiation and hypertrophy. (**a**) Representative images of Alcian Blue staining show chondrocytes (stained in blue) from bone marrow cells cultured with TGF-β3 for 14 days. (**b**) Quantification of chondrocyte differentiation. OD, optical density. ns, not significant. n=3. (**c**) Representative images of immunofluorescence staining of COLX positive cells (green) from histological sections of E18.5 mouse femurs. (**d**) *COLX* and *Mmp13* mRNA expression from bone marrow cells cultured with TGF-β3 for 14 days. ns, not significant. n=3.

Figure S6

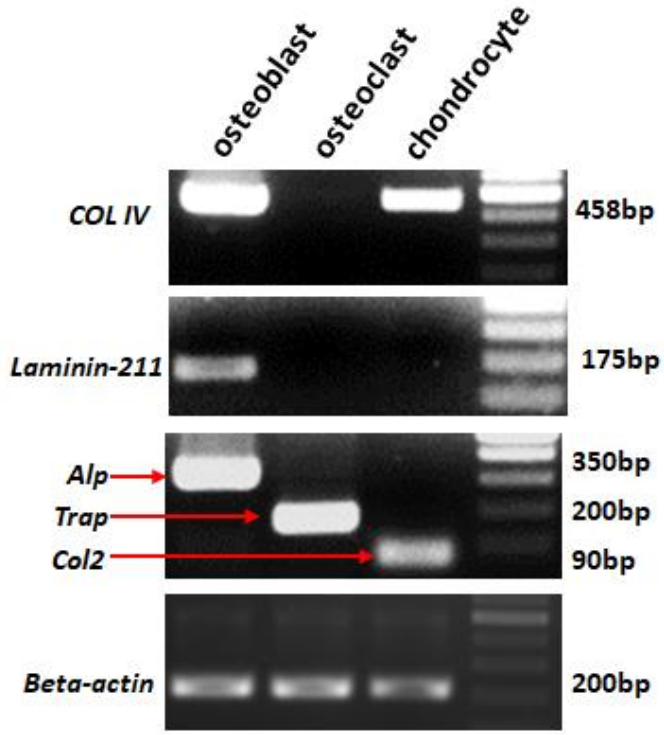

Fig. S6. The expression of COLIV and Laminin-211 in osteoblast, osteoclast, and chondrocyte cells. Representative gel showing the expression of *COLIV* and *Lamini-211* in osteoblasts, osteoclasts and chondrocytes, respectively.

Figure S7

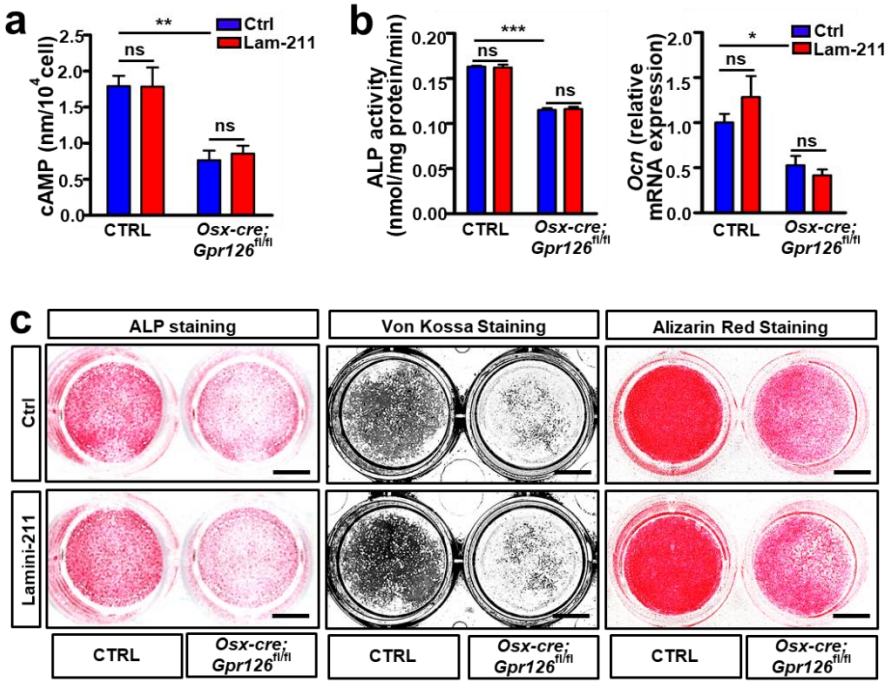

Fig. S7. *Laminin-211* was not an activating ligand of *Gpr126* to regulate osteoblast differentiation and mineralization under static conditions. (**a**) Laminin-211 (Lam-211) had little effect on cAMP level in control or *Gpr126* deletion osteoblasts. Lam-211 was coated on 24-well plates and then the BMSCs were seeded for differentiation. After 14 days, the cells were harvested and subjected to cAMP ELISA assay. **p < 0.01. ns, no significant difference. n=3. (**b**) Lam-211 had little effect on ALP enzyme activity (n=3) and *Ocn* mRNA expression (n=2) in osteoblasts. *p < 0.05, ***p < 0.001. ns, not significant. (**c**) Lam-211 has little effect on osteoblast differentiation and mineralization in osteoblasts. ALP staining, Von Kossa staining, and Alizarin Red staining of BMSCs after 7, 14 and 21 days of differentiation, respectively, while treated with or without Lam-211. Scale bars, 5mm.

Figure S8

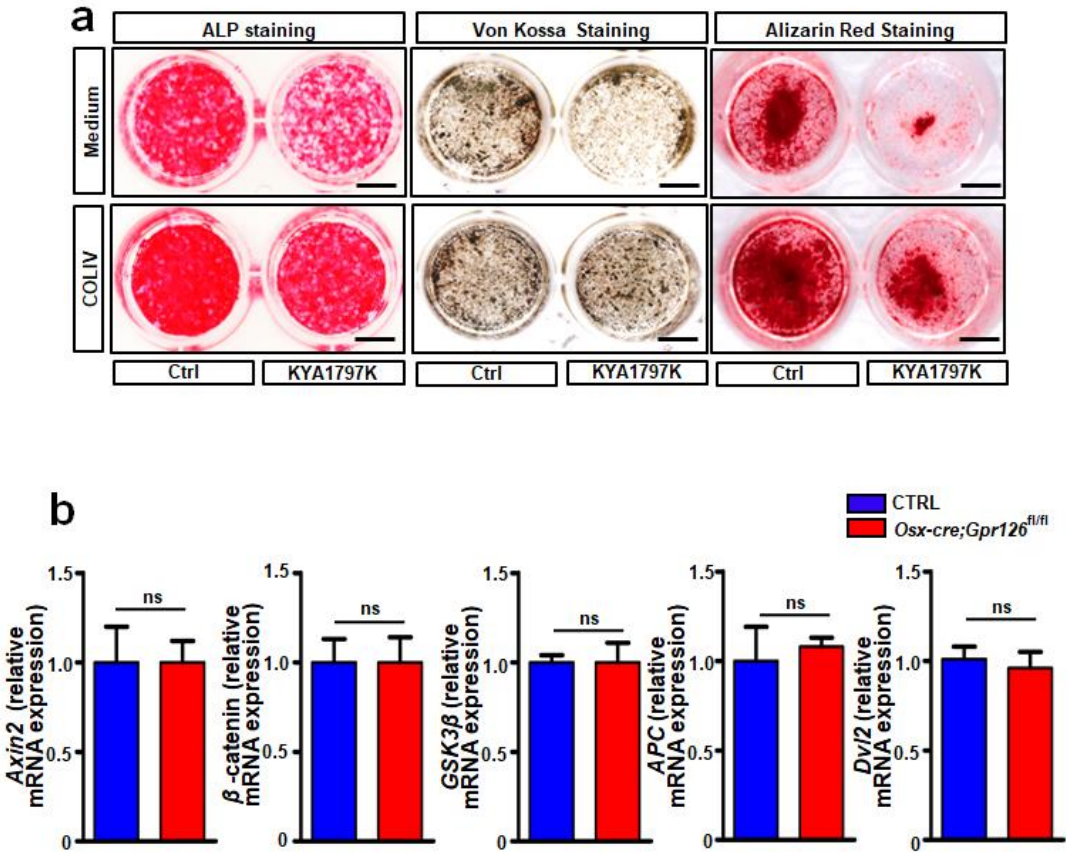

Fig. S8. The selective Wnt/β-catenin inhibitor KYA1797K had little effect on COLIV-induced osteoblast differentiation and mineralization. (**a**) COLIV stimulated osteoblast differentiation and mineralization; however, the selective Wnt/β-catenin inhibitor, KYA1797K, had little effect on COLIV-induced osteoblast differentiation and mineralization. ALP staining, Von Kossa staining, and Alizarin Red staining of BMSCs was performed after 7, 14 and 21 days of differentiation, respectively. Scale bars, 5mm. (**b**) Knocking-out *Gpr126* had little effect on Wnt/β-catenin downstream target gene expression in osteoblast cells. After the Ctrl (Osx-Cre) BMSCs and *Osx-Cre*;*Gpr126*$^{fl/fl}$ BMSCs were differentiated into osteoblasts for 7 days, the cells were harvested and total RNA was extracted for Real-time PCR.

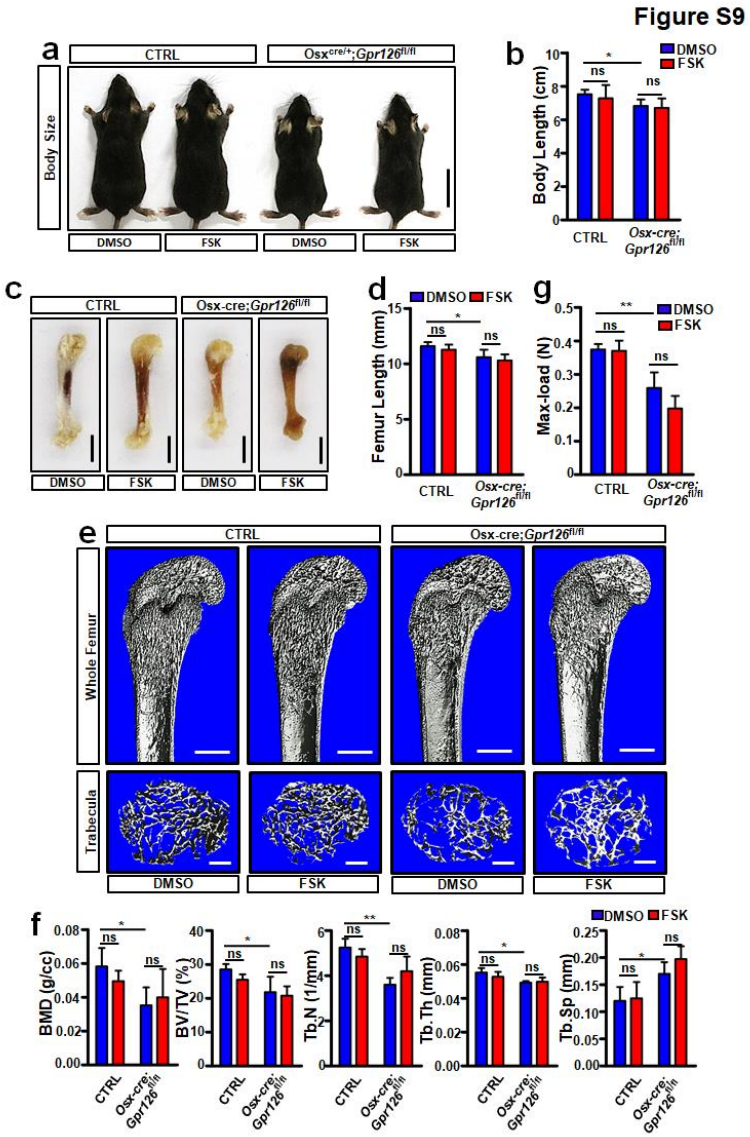

Fig. S9. Administration of FSK had little effect on the body length, femur bone length, bone mass, and bone strength of *Osx-Cre;Gpr126*$^{fl/fl}$ mice.

Osx-Cre;*Gpr126*$^{fl/fl}$ mice and Ctrl littermates (n =6 mice/group) were injected daily with vehicle or 200 μg/kg FSK from P5 to P30. The mice were then sacrificed for body length, bone length, bone mass and bone strength analysis. (a and b) Representative images of Osx-Cre;*Gpr126*$^{fl/fl}$ mice and Ctrl littermates treated with vehicle or 200 μg/kg FSK (a). The body length was measured (b). ns, not significant, *p < 0.05. Scale bars, 2 cm. n=6. (c and d) Representative femur bone images of Osx-Cre;*Gpr126*$^{fl/fl}$ mice and Ctrl littermates treated with or without 200 μg/kg FSK (c). The femur bone length was measured (d). *p < 0.05. Scale bars, 2 cm. n=6. (e and f) Representative μCT images of femurs from 1-month old Osx-Cre;*Gpr126*$^{fl/fl}$ mice and Ctrl littermates treated with 200 μg/kg FSK. The proximal femur (top) and trabecular bone of the femur metaphysis (bottom) are presented (e). Quantitative μCT analysis of femur trabecular bone parameters (f). Scale bars: 500 μm (top); 200 μm (bottom). *p < 0.05, **p < 0.01. n=6. (g) Maximal loading of humeral diaphysis from 1-month-old mice by three-point bending assay. Max-load, maximal load. *p < 0.05, **p < 0.01. n=6. Photo credit: Liang He, East China Normal University

Figure S10

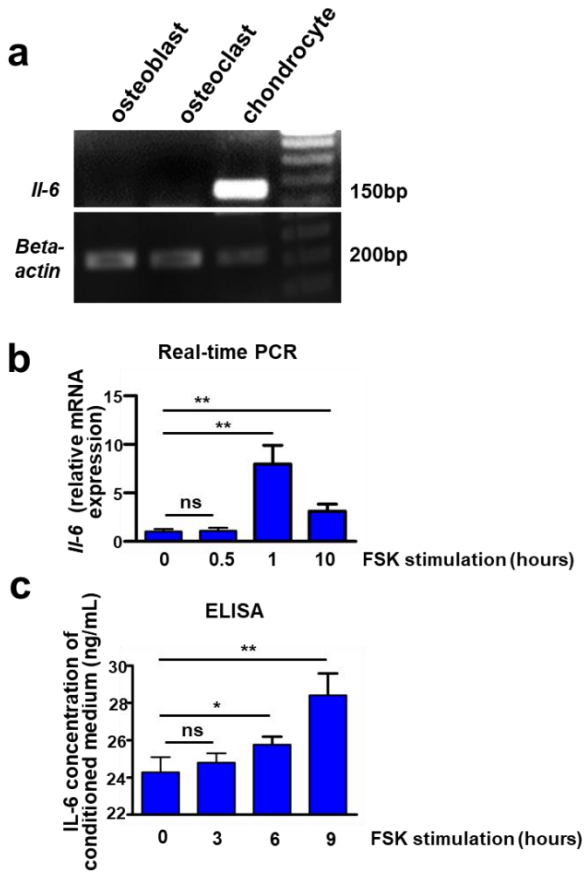

Fig. S10. The expression of IL-6 was increased in chondrocytes treated by FSK. (**a**) *Il-6* was expressed in chondrocytes but not osteoblasts and osteoclasts. (**b**) The relative mRNA expression of *Il-6* in chondrocytes from wild type mouse articular cartilage at 0 min, 30 min, 1 hour, and 10 hours of 10uM FSK treatment. ns, not significant, **p < 0.01. n=3. (**c**) The protein level of IL-6 in conditioned medium of chondrocytes from wild type mouse articular cartilage after 10 μM FSK treatment for indicated times. ns, not significant, *p < 0.05, **p < 0.01. n=3